

## Thermodynamics and Kinetic Study for Removal of Orange-G Dye from Aqueous Solution by Nano Composite

Amir. F. Dawood AL-Niaimi, Reem Marwan Kailan

<sup>12</sup>Department of Chemistry/ College of Science/ university of Diyala/ Diyala/Iraq.

### KEYWORDS

COMBI method, Stunting, Pamekasan

### ABSTRACT

In this study, where graphene oxide was prepared by Hummer method, while copper oxide was prepared in the green way using (capparies spinosa) plant extract as a reducing agent, these oxides were diagnosed as well as the binary nanocomposite by several techniques including Fourier Transform Infrared Spectroscopy (FTIR), X-rays diffraction, and field Emission scanning electron microscopy (FESEM), after that the superimposed (GO/CuO) was used to adsorbent the orange G dye (Orange - G) from its aqueous solutions, A number of factors affecting adsorption were studied (equilibrium time, surface weight, pH, concentration effect, temperature). The results showed that the ideal time for adsorption of the orange dye (orange-G) on the surface of the nanocomposite (GO/CuO) was (30min), the best ideal weight for dye removal was (0.05gm), the best concentration was (20ppm), and the best acid function was (pH=2). After that, the adsorption kinetics were also studied by applying the pseudo first and second order of adsorption. The results showed that the adsorption process follows the false second-order kinetics. The thermodynamic functions of the removal process were also studied, and it was found that the value of ( $\Delta H$ ) is negative for the surface of the composite (GO/CuO) with dye. Meaning the adsorption process is exothermic, and that the  $\Delta G^0$  has negative value, meaning that the adsorption processes occur spontaneously. positive  $\Delta S^0$  values indicate that the molecules are becoming less bound

### 1. Introduction

The physical, chemical, or biological effects of human industrial or social activity define pollution as any detrimental alteration in the environment. Pollutants, which are the factors responsible for environmental pollution, are identified as {4,5}. Pollution is a significant issue that can arise from the technological advancements accompanying modern life, affecting both humans and the environment. Pollution can manifest in various forms, encompassing air, water, and soil pollution. Organic compounds, particularly dyes, are often pollutants that are extensively released into the aquatic environment. These compounds are known to be hazardous, poisonous, and carcinogenic, posing risks to human health and the aquatic ecosystem {7}. The basic ingredients utilized in the production of these colors are inherently carcinogenic substances, including aniline, benzidine, and other amino compounds. The dyes can undergo breakdown during certain biological processes, resulting in changes in their color and form. Adsorption is a prevalent technique in the field of physics and chemistry for eliminating contaminants. Hence, it is imperative to eliminate the dye from wastewater to save the ecology and promote human well-being. Adsorption is the process by which molecules, ions, or atoms from one substance gather on the surface of another substance. Adsorption phenomena can be categorized based on the nature of the forces between the surface of molecules, atoms, or ions that are adsorbed onto the surface of the adsorbent. These categories include physisorption and chemisorption. The variables that influence adsorption include the acidity of the surface, the surface area and type of the adsorbent, the characteristics of the item being adsorbed, the temperature, and the solvent used.

Dyes are chromatic chemical compounds employed to impart their hue to a substrate, thereby integrating with it through dyeing, printing, or surface coating techniques. We can categorize dyes based on their structure, chromophore group, or how their ions change when dissolved in water-based solutions. We classify dyes into two primary types based on their charge: ionic dyes and non-ionic dyes. We can categorize ionic dyes as cationic dyes, also referred to as basic dyes, because they possess positive ions. Anionic dyes are characterized by the presence of negative ions due to an abundance of (OH) ions when they are dissolved in water {17}. Orange G dye is a common anionic dye that dissolves in water. It is frequently used in the paper industry and has harmful effects on biological organisms [26]. The chemical formula is  $(C_{16}H_{10}N_2Na_2O_7S_2)$  {27}. Graphene has garnered significant attention due to its remarkable ability to enhance the properties of polymer nanocomposites. Graphene's exceptional mechanical, thermal, and electrical properties stem from its honeycomb-like structure, which consists of a single carbon atom. Additionally, graphene exhibits high electronic abundance in its structural structure, further contributing to its desirable characteristics. The copper oxide nanoparticle exhibits semiconductor properties. The (CuO) nanoparticle is a solid powder that cannot dissolve in water ( $H_2O$ ) but may dissolve in ( $NH_4Cl$ , dilute acid, and ammonia solution at a slow rate). Green chemistry is a field that emphasizes the creation of desirable products without the formation of harmful intermediate byproducts during chemical reactions. The incorporation of green chemistry concepts into nanotechnology has resulted in the discovery of environmentally sustainable reagents that have multiple functions, acting both as reducing agents and capping agents [23, 24]. Plants have been used to synthesize various nanoparticles, including those derived from leaf extract, fruit, tea, and flower extract. {25}

## Experimental

### Preparation of GO

The synthesis of nano graphene oxide was carried out using the modified Hummer method, with a starting material of (2 grams). The graphite was combined with (50 mL of  $H_2SO_4$ ) in a (1000-mL) beaker using a magnetic stirrer. The mixture was then placed in an ice bath at a temperature of ( $0^\circ C$ ) . Next, (2grams) of sodium nitrate were added to the mixture. Gradually and steadily, continue to add the substance while stirring constantly for a duration of (20 minutes). Following this, progressively introduce (6grams) of ( $KMnO_4$ ) over a period of (2 hours) . Next, introduce (100 milliliters) of non-ionic water to increase the temperature to ( $98^\circ C$ ) for a duration of (30 minutes) . Following this, add an additional (400 milliliters )of water to complete the process. After the oxidation process is complete, (20mL) of hydrogen peroxide ( $H_2O_2$ ) is added. The mixture is then filtered and washed using a solution of 5% hydrochloric acid (HCl) and non-ionic water. Finally, the mixture is dried at a temperature of (  $70^\circ C$  )for a duration of (4 hours). {28, 29}

### Preparation of CuO

#### Preparation of Capparis spinosa aqueous extract

We gathered the foliage of the Capparis spinosa plant from a specific location in Diyala governorate. It was meticulously cleansed of any particulate matter, thoroughly rinsed multiple times with water, and subsequently dried. A (1000ml) beaker was filled with (5g) of Capparis plant. Then, (400 ml) of non-ionic water was added to the beaker. The mixture was heated to ( $70^\circ C$ ) for (30 minutes) . After that, it was filtered, and the remaining liquid was removed using a centrifuge at (4000 rpm) for 4 minutes.

#### Preparation of CuO

A solution containing (3 grams) of ( $Cu(NO_3)_2 \cdot 3H_2O$ ) was dissolved in (1000 milliliters )of non-ionic

water. Then, at room temperature, (30 milliliters) of plant extract were gradually added to the solution while continuously stirring. The pH of the mixture was adjusted by increasing the temperature to (50<sup>0</sup>C) and adding (20 milliliters) of NaOH. The solution was then filtered and washed multiple times with non-ionic water. Ethanol was added, and the mixture was dried at a temperature of (90<sup>0</sup>C) for 2 hours. {30}.

### Preparation of GO/CuO

The bi nano composites were synthesized by dispersing (1g) of graphene oxide (GO) in (200ml) of non-ionic water using an ultrasonic water bath at room temperature for (1 hour). Subsequently, (0.7g) of copper oxide (CuO) was added to the GO solution and stirred for (1 hour). Subsequently, the mixture is subjected to centrifugation to achieve separation, followed by drying at a temperature of (90<sup>0</sup>C) for a duration of (4 hours) .{ 31}

### Determine the calibration curve for the orange G

The dye orange G was made as a solution, and from this solution, various solutions with varying concentrations were prepared. The concentrations were determined using a (UV-Vis) spectrophotometer, which measures light absorption in the range of 200-800nm. A quartz cell with a cross area of (1cm) was used for the measurements. The wavelength was adjusted to the point of maximum absorption. The analysis revealed that the orange G dye has a wavelength ( $\lambda_{max}$ ) of 477nm, as depicted in **figure (1)**. The molar absorbance coefficient was determined by creating a graph of absorbance vs concentration, as shown in **Figure (2)**, and using the Lambert-Beers law.

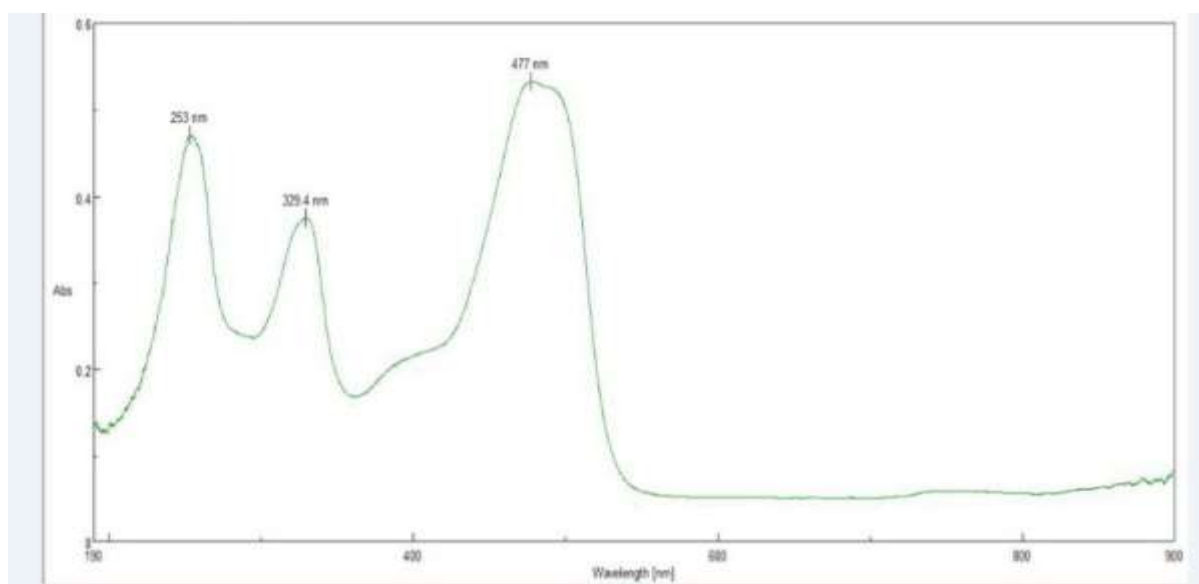
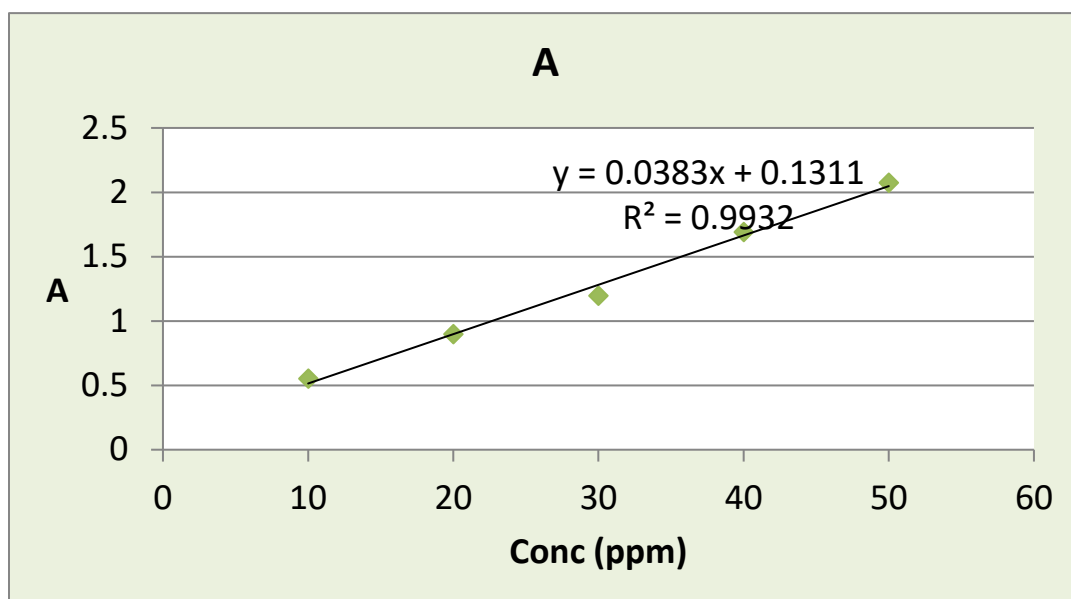


(Figure 1) (UV-Vis) absorption spectrum of Orange -G

(Figure 2) Calibration Curve For Orange- G dye



Determine the optimum conditions for adsorption

#### Equilibrium time

In order to ascertain the time needed for equilibrium to be reached between the adsorbent and the adsorbent surface, five volumetric bottles with a capacity of (150ml) were utilized. Each bottle contained the same volume of orange G dye, with a concentration of (10ppm). An amount of (0.01 grams) of the GO/CuO surface was placed in each bottle and then placed in a shaker at a temperature of (25°C). Subsequently, the bottles were intermittently removed (at intervals of (10, 20, 30, 40, and 50) and subjected to centrifugation. Following this, the absorbance of the dye was measured at its peak wavelength of (477nm). The findings indicate that the time needed to reach equilibrium for each case is (30 minutes). refer to Table( 2-1) and Figure (3-a) .{ 32}

(GO/CuO)		
Time(min)	C <sub>e</sub> (ppm)	R%
0	10	0
10	11.71	18.6
20	11.69	18.8
30	10.62	26.2
40	11.76	18.3
50	11.21	22.1

(Table 0-1) Effect of equilibrium time on the removal of orange-G dye

#### Effect of Weight

The adsorbent surface is weighed by taking a sample of( 0.01-0.05 g ) and depositing it in bottles with a volume of (150 ml). Each bottle contains (30 ml) of dye with a concentration of (10 ppm). This is done simultaneously for all samples. Subsequently, the bottles were introduced into a shaker operating at a temperature of (25°C), followed by the placement of the solutions into the centrifuge. Subsequently, the absorbance was measured at their respective wavelengths. It was determined that the optimal surface adsorbent, weighing (0.05g), is represented in table (2-2) and figure (3-b).{ 32}

wt	C <sub>e</sub> (ppm)	R%
----	----------------------	----

0.01	0.027	99.81
0.02	0.024	99.83
0.03	0.021	99.85
0.04	0.022	99.84
0.05	0.017	99.88

(Table 0-2) Effect of weight on the removal of orange-G dye

#### Effect of Concentration

We created various concentrations of orange G dye ranging from (10 to 50 ppm). From each concentration, we took (30 ml) of dye and added (0.05g ) of GO/CuO to each bottle. The bottles were placed in a shaker at a temperature of( 25°C). After the separations were conducted, the absorbance was measured at the specific wavelength of the dye. The optimal removal efficiency was seen at a concentration of (20ppm), as indicated in **Table (2-3)** and **Figure (3-c)**.{ 33 }

GO/CuO		
C <sub>0</sub> (ppm)	C <sub>e</sub> (ppm)	R%
10	7.50	47
20	7.05	69
30	21.53	30
40	28.90	34
50	29.80	44

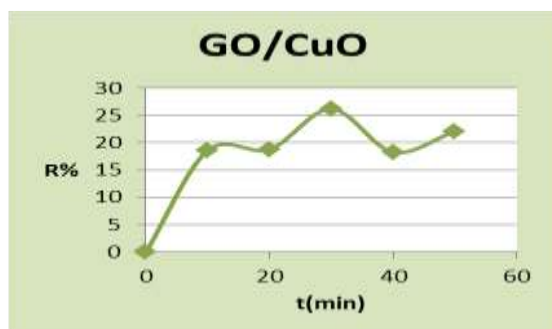
(Table 0-3) Effect of concentration on the removal of orange-G dye

#### Effect of pH

The weight of (0.05g) of GO/CuO was measured once all parameters were set. Subsequently, the weight was combined with (30ml) of dye and subjected to several acid concentrations (2, 10, 12). Subsequently, the bottles were inserted into a shaker at a temperature of (25°C). These solutions were then transferred to a centrifuge and filtered. The absorbance of the solutions was measured using a (UV-Vis) spectrometer. The optimal acid value was found to be( pH= 2) for the dye **table (2-4)** and **Figure(3-d)**.

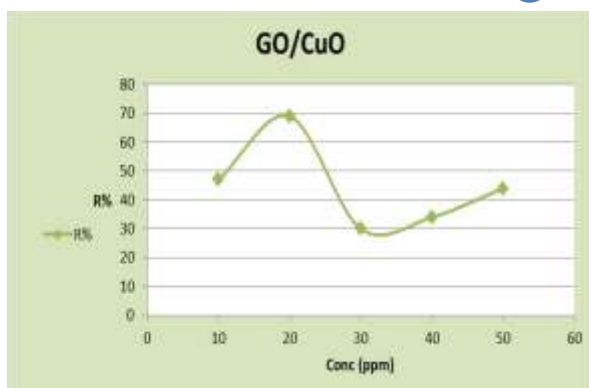
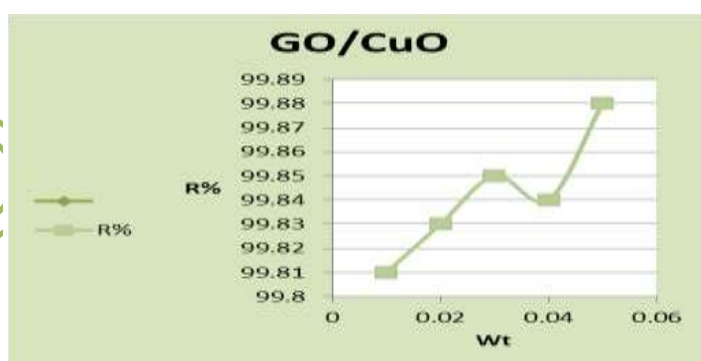
GO/CuO		
PH	C <sub>e</sub> (ppm)	R%
2	8.66	39.86
10	14.36	0.27
12	12.21	15.20

(Table 0-4) Effect of pH on the removal of orange-G dye



a- effect of equilibrium time

b- effect of weight



c- effect of concentration

d- effect of pH

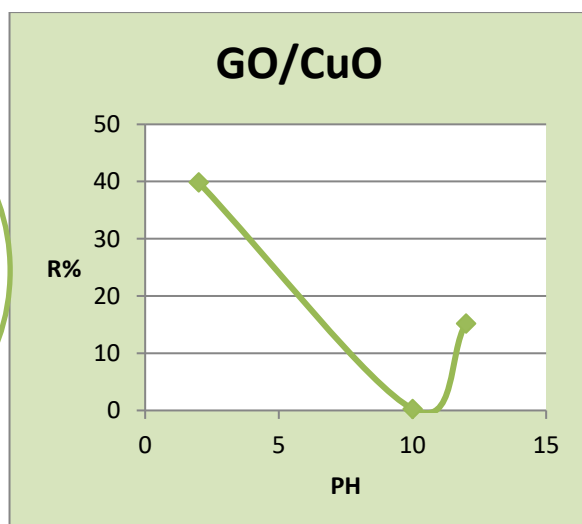


(Figure 3) Effect (a- equilibrium time ,b-weight ,c-concentration ,d-pH)

### Determine of adsorption Isotherm

Various diluted solutions of dye (orange -G) were made with varying concentrations (10, 20, 30, 40, 50 ppm) in volumetric bottles with a capacity of (150ml). Next, a volume of (30ml) was extracted from each of the various concentrations and transferred into bottles with a capacity of (150ml). Then, an ideal weight of (0.05g) was added separately to each bottle from the surface of the GO/CuO mixture. Subsequently, they were introduced into a shaker apparatus under carefully regulated temperature conditions. Once the surface with dye reached equilibrium, the separation process was conducted and the concentrations of the solutions were determined using a (UV-Vis) spectrometer. Subsequently, the values for ( $C_e$  ppm) and ( $Q_e$  mg/g) were computed using the following mathematical equation:

$$Q_e = \frac{C_0 - C_e V_{\text{solution}}}{M_{\text{adsorbent}}} \quad \text{Equation 1}$$

$Q_e$  represents the amount of substance that was adsorbed, measured in milligrams per gram.  $C_e$  refers to the remaining concentration of the substance at equilibrium time, measured in parts per million.  $V_{\text{sol}}$  represents the entire volume of the adsorbent solution, measured in liters.  $C_0$  is the initial concentration of the adsorbent, also measured in parts per million.  $M$  represents the weight of the adsorbent surface.

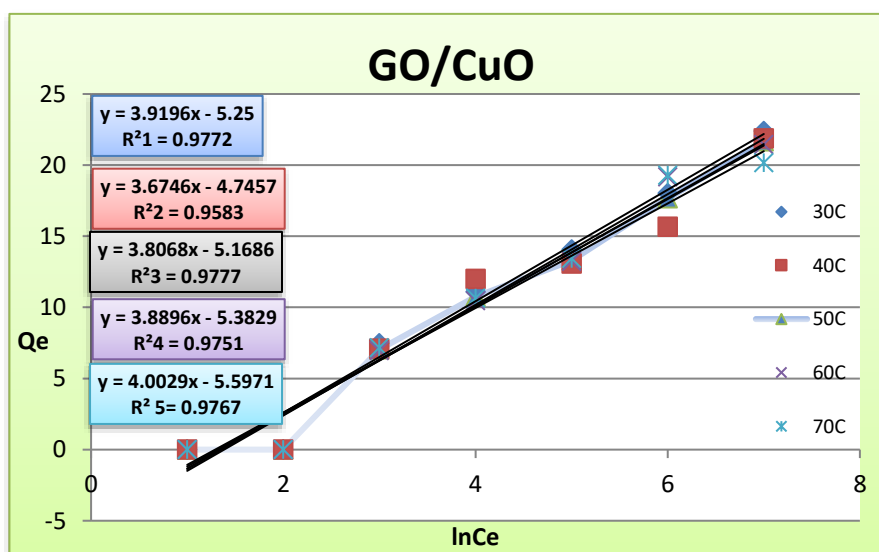


(Figure 4) effect of temperature change on the adsorption capacity of orange-G dye on the surface of the composite (GO/CuO)

### Thermodynamic

The thermodynamic study of the adsorption process gives a general idea of the various thermodynamic functions such as enthalpy ( $\Delta H$ ), randomness ( $\Delta S$ ), and spontaneity of the system ( $\Delta G$ ). as the study is carried out at different temperature. The value of ( $\Delta H$ ) can be calculated by plotting ( $\ln X_m$ ) against the reciprocal of temperature figure (5) table (2-5) and based on the following Vant Hoff equation.

From the slope of the linear relationship  $\Delta H$  is calculated{34}:  $\ln x_m = \frac{-\Delta H}{RT} + \text{conc}$  Equation 2



so/  $\ln X_m$ : is the logarithm of the maximum amount adsorbed (mg/g),  $\text{conc}$ : constant Vant Hoff equation,  $T$ : temperature (K),  $R$ : is the general constant for gases. The change in the value of the compression energy ( $\Delta G$ ) is calculated through the following{35}:

$$\Delta G^0 = -RT \ln K_c \quad \text{Equation 3 ,}$$

Thermodynamic functions can be calculated using the freundlich constant{36}

$$k_c = k_f * 10^3, k_f : \text{Freundlich constant .}$$

Thus, it was possible to obtain the values of the entropy change as by applying the

$$: \Delta G^0 = \Delta H - T \Delta S^0 . \quad \text{Equation 4}$$

GO/CuO					
$C_o$	$T(^{\circ}\text{C})$	$T(\text{K})$	$1/T$	$X_m$	$\ln X_m$
50ppm	30	303	0.0033	22.3	3.10
	40	313	0.00319	21.8	3.08
	50	323	0.00309	21.6	3.07
	60	333	0.003	21.4	3.06
	70	343	0.00291	22.1	3.0

(Table 0-5) values of maximum adsorption amount ( $\ln X_m$ ) and different temperature of orange –G dye

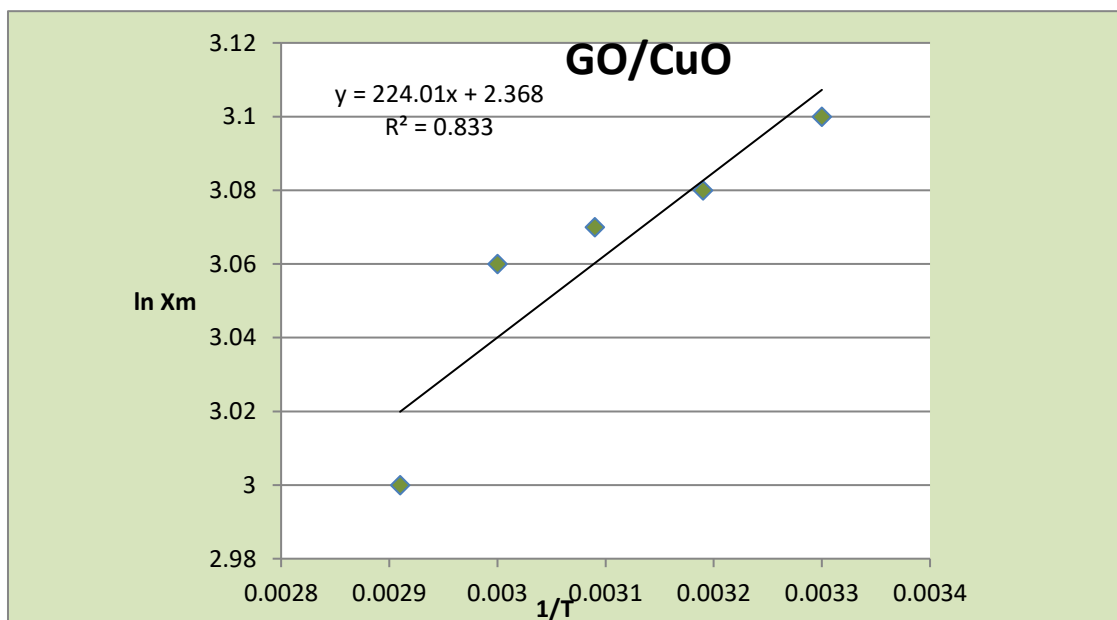


(Figure 5) (Maximum adsorption amounts ( $\ln X_m$ ) and different temperatures of orange G dye )

GO/CuO					
$C_o$	$T(^{\circ}\text{C})$	$T(\text{K})$	$1/T$	$KF$	$\ln Kc$
50 ppm	30	303	0.0033	0.681	6.523
	40	313	0.00313	0.697	6.546



	50	323	0.00309	0.675	6.514
	60	333	0.003	0.664	6.498
	70	343	0.00291	0.662	6.495

(Table 0-6) ( values of the equilibrium constant  $\ln K$  and different temperature for orange G dye)

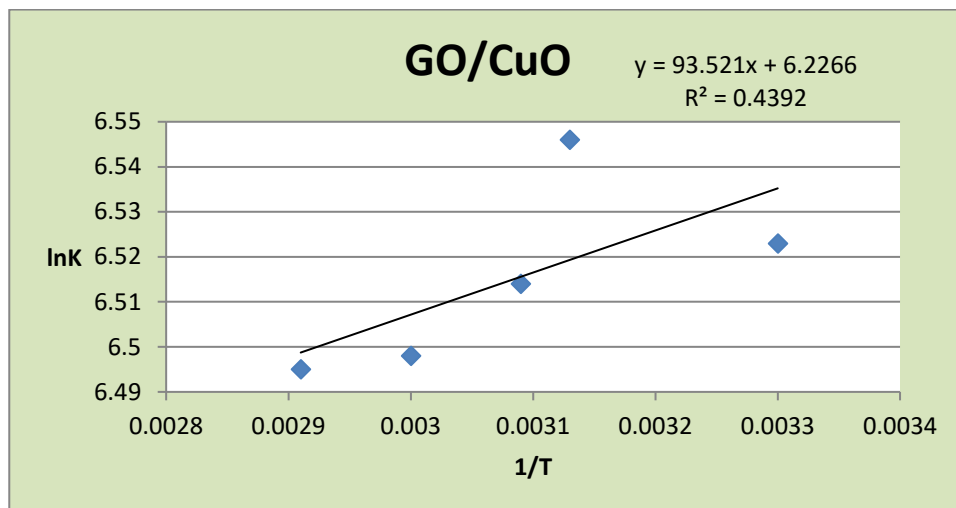


(Figure 6) (values of the equilibrium constant  $\ln K$  and different temperatures  $1/T$  of the orange G dye)

GO/CuO						
Co	Thermodynamic Function	30°C	40°C	50°C	60°C	70°C
50(ppm)	$\Delta^0 G(KJ/mol)$	-16.43	-17.03	-17.49	-17.90	-18.52
	$\Delta H(KJ/mol)$	-1.862				
	$\Delta^0 S(J/mol.K^{-1})$	0.06	0.0484	0.0483	0.0481	0.0485

(Table 0-7) (values of the thermodynamic functions for the adsorption of the orange G dye)

### Determination of adsorption Kinetic

The surface kinetics of the (orange- G) dye on the secondary composite were monitored. A sample weighing (0.05 grams) was extracted from the mixture of graphene oxide (GO) and copper oxide (CuO). This sample was then added to bottles, each containing (150 milliliters), along with (30 milliliters) of dye solution with a concentration of (20ppm). Subsequently, these bottles were placed in a shaker for further processing. samples were collected at various time intervals (6, 12, 18, 24, and 30 minutes) for the GO/CuO material. Subsequently, the sequence of interaction between the adsorbent and adsorbent surface was established. This was accomplished by utilizing the equation from the first incorrect rank (2) [table\(2-8\) figure\(7\)](#) and the second incorrect rank (3) [table\(2-8\) figure\(8\)](#).

$$\ln(q_e - qt) = \ln q_e - K_1 t \quad \text{Equation 5}$$

qt: it is the amount of adsorbed material at different times, qe: is the a mount of adsorbed material at equilibrium (mg/g) and when drawing ln( qe-qt) versus time, the slope represents (-K) and the intercept represents (ln qe).

$$\frac{t}{qt} = \frac{1}{K_2 q_e^2} + \frac{1}{q_e} t$$

**Equation 6**

The value of (K<sub>2</sub>,q<sub>e</sub>) are obtained directly from the slope and intercept when plotting t/qt against time. **K<sub>2</sub> = (slope)<sup>2</sup>/intercept**, K<sub>2</sub>: represents the initial pseudo second order adsorption constant (g/mg.min), q<sub>e</sub>: is the amount of adsorbed substance at equilibrium (mg/g).

GO/CuO				
T=30				
Time	C <sub>e</sub> (ppm)	qt	Ln(qe-qt)	t/qt
6	6.624	10.077	0.022	0.595
12	7.652	9.460	0.494	1.268
18	7.530	9.534	0.448	1.887
24	9.096	8.594	0.918	2.792
30	7.78	9.384	0.539	3.856
T=40				
6	13.266	6.092	1.772	0.984
12	12.198	6.733	1.656	1.782
18	11.671	7.049	1.595	2.553
24	12.044	6.825	1.638	3.516
30	7.733	9.412	0.940	3.187
T=50				
6	10.373	7.828	1.071	0.767
12	8.976	8.666	0.732	1.385
18	8.812	8.764	0.683	2.054
24	8.830	8.754	0.688	2.742
30	7.349	9.642	0.113	3.111
T=60				
6	8.436	8.990	-0.385	0.667
12	8.253	9.100	-0.562	1.318
18	7.715	9.423	-1.386	1.910
24	7.684	9.441	-1.469	2.542
30	7.120	9.78	-0.400	3.067
T=70				
6	8.945	8.685	0.662	0.691
12	8.906	8.708	0.652	1.379
18	8.214	9.123	0.405	1.973
24	7.608	9.487	0.131	2.531
30	7.396	9.614	0.009	3.121

(Table 0-8) (values of the pseudo first- second order equations for the adsorption of orange G dye)

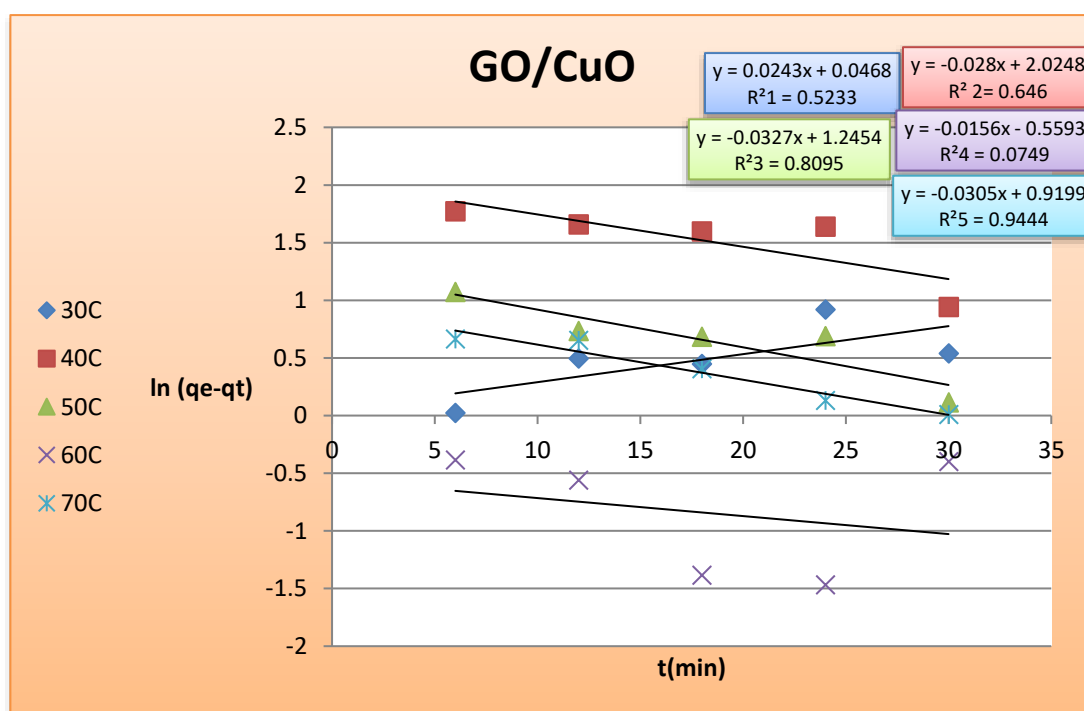


(Figure 7) pseudo-first order kinetics of adsorption of orange G dye onto the surface of the composite GO/CuO

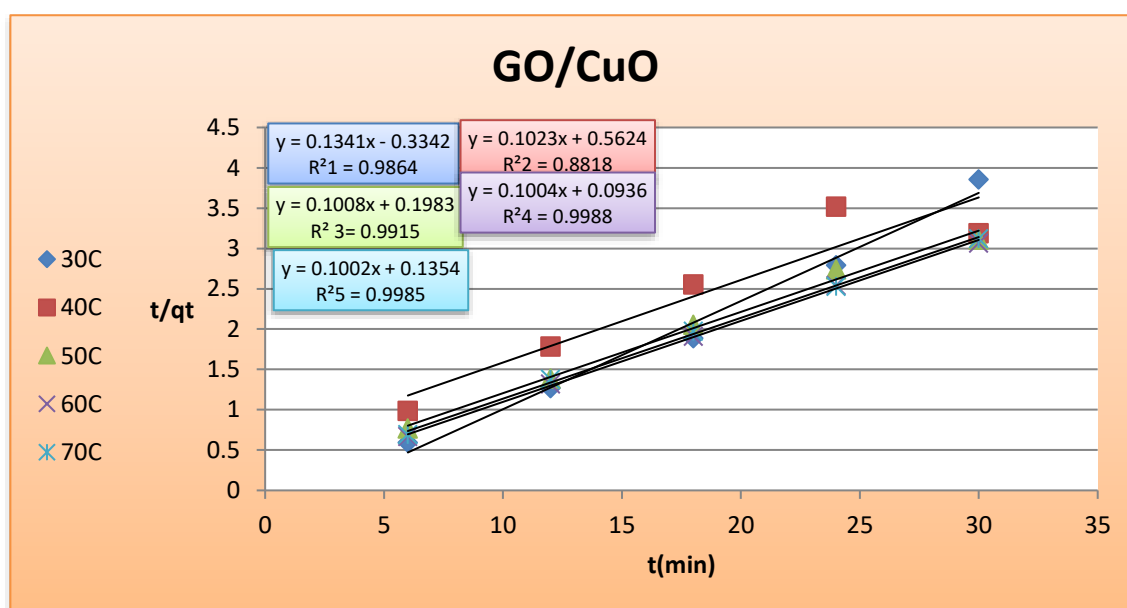


(Figure 8) pseudo-second order kinetics of adsorption of orange G dye onto the surface of the composite GO/CuO

GO/CuO							
C <sub>o</sub> (20ppm)	T <sub>c</sub>	First			Second		
		K1	q <sub>e</sub>	R <sup>2</sup>	K <sub>2</sub>	q <sub>e</sub>	R <sup>2</sup>
	30	-0.024	1.047	0.5233	0.053	7.457	0.9864
	40	0.028	7.574	0.646	0.018	9.775	0.8818
	50	0.032	3.474	0.8095	0.051	9.920	0.9915
	60	0.015	0.571	0.0749	0.107	9.960	0.9988

	70	0.030	2.509	0.9444	0.074	9.980	0.9985
--	----	-------	-------	--------	-------	-------	--------

(Table 0-9) first and second order pseudo variables for the adsorption of orange G dye on a surface GO/CuO)

## Characterization

### FTIR (Fourier Transform Infrared) spectroscopy

#### FTIR (GO)

Figure (9) illustrates multiple bands corresponding to functional groups in GO. A cluster of bonds is observed at the region of ( $3348.03\text{cm}^{-1}$ ), indicating the presence of carboxylic acid groups with potential adsorption of water molecules on the surface. Additionally, an absorption band at ( $1717.51\text{cm}^{-1}$ ) signifies the presence of carbonyl groups. The presence of (C=O) groups, specifically carbonyl and carboxyl groups, unequivocally signifies the creation of graphene oxide. Additionally, there is an absorption band observed at the specific wavelength of ( $1187.78\text{ cm}^{-1}$ ) . It is a member of the (C=C) group that is linked to structural vibrations. The unoxidized graphene bands are observed within the range of ( $1049.63\text{-}869.65\text{cm}^{-1}$ ) and are attributed to the alkoxy group or Bending COOH group and epoxy group.

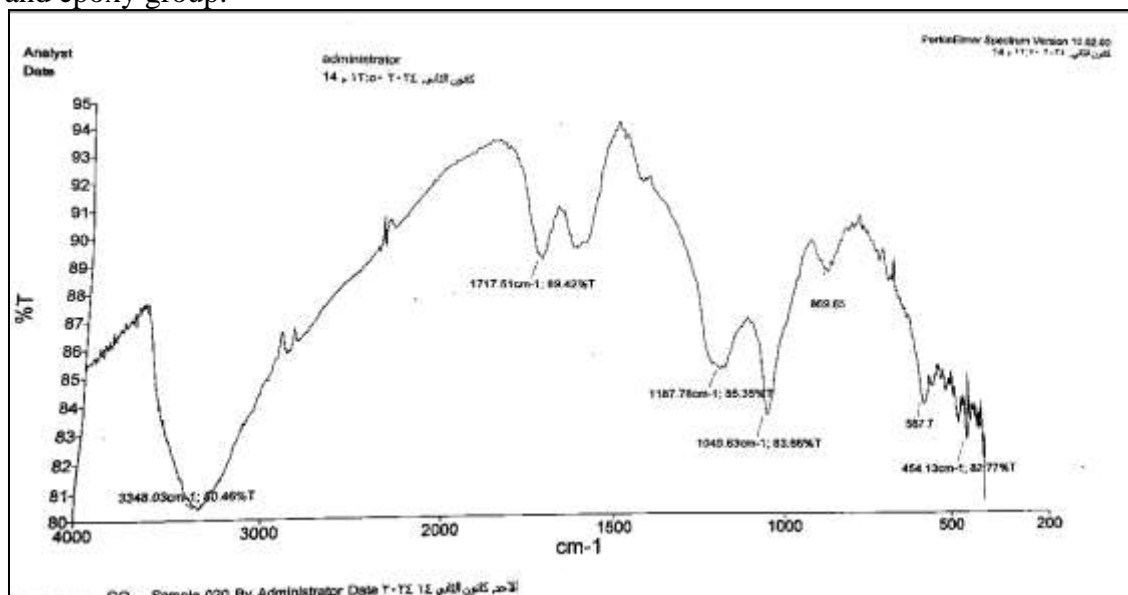


(Figure 9) infrared spectrum of the (GO)

#### FTIR (CuO)

(Figure 10) shows the Fourier Transform Infrared (FTIR) spectra of Copper Oxide (CuO) across the range of ( $200\text{-}4000\text{cm}^{-1}$ ), measured at ambient temperature. The peak observed at a wavenumber of ( $3398.07\text{ cm}^{-1}$ ) corresponds to the stretching of the N-H bond, which is likely attributed to the presence of an amino acid. The presence of peaks at ( $506, 599\text{cm}^{-1}$ ) suggests the creation of CuO nanostructure and CuO stretching. The peaks detected within the range of ( $1384, 1629\text{cm}^{-1}$ ) are indicative of O-H bending and C=C stretching. The peaks at ( $876.93$  and  $984\text{ cm}^{-1}$ ) can be attributed to the bending of C-O and C-H bonds. {1}{2}

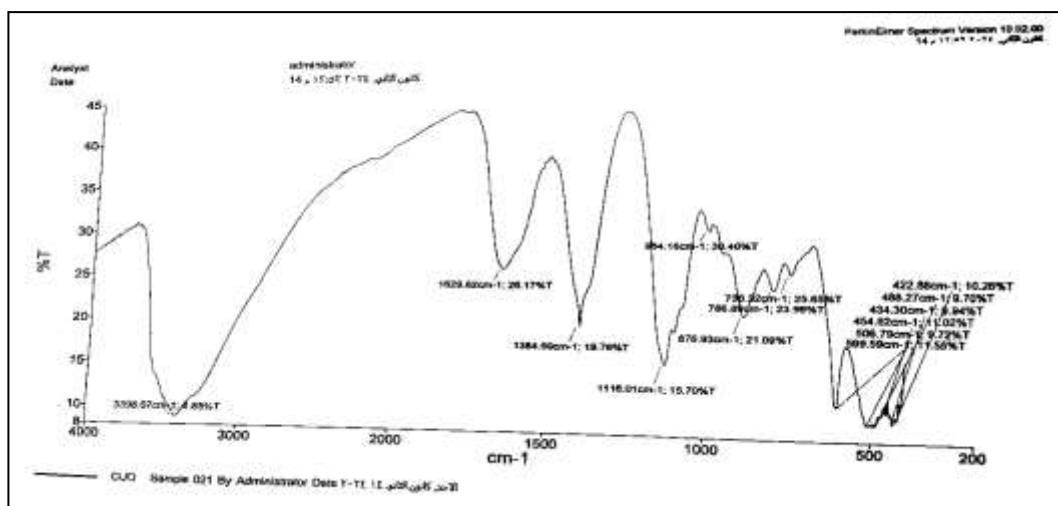


(Figure 10) infrared spectrum of the (CuO)

### FTIR (GO-CuO)

The presence of CuO is indicated by the emergence of beams at coordinates (660.68, 434.02 cm⁻¹), as seen in Figure (11). An absorption peak is observed at the region (1628.22 cm⁻¹) corresponding to the C=C functional group. Additionally, several peaks are detected, indicating the existence of both graphene oxide (GO) nanoparticles and copper oxide (CuO) nanoparticles. The O-H group exhibits an elastic bundle at the specific region of 3432.52 cm⁻¹. {3}

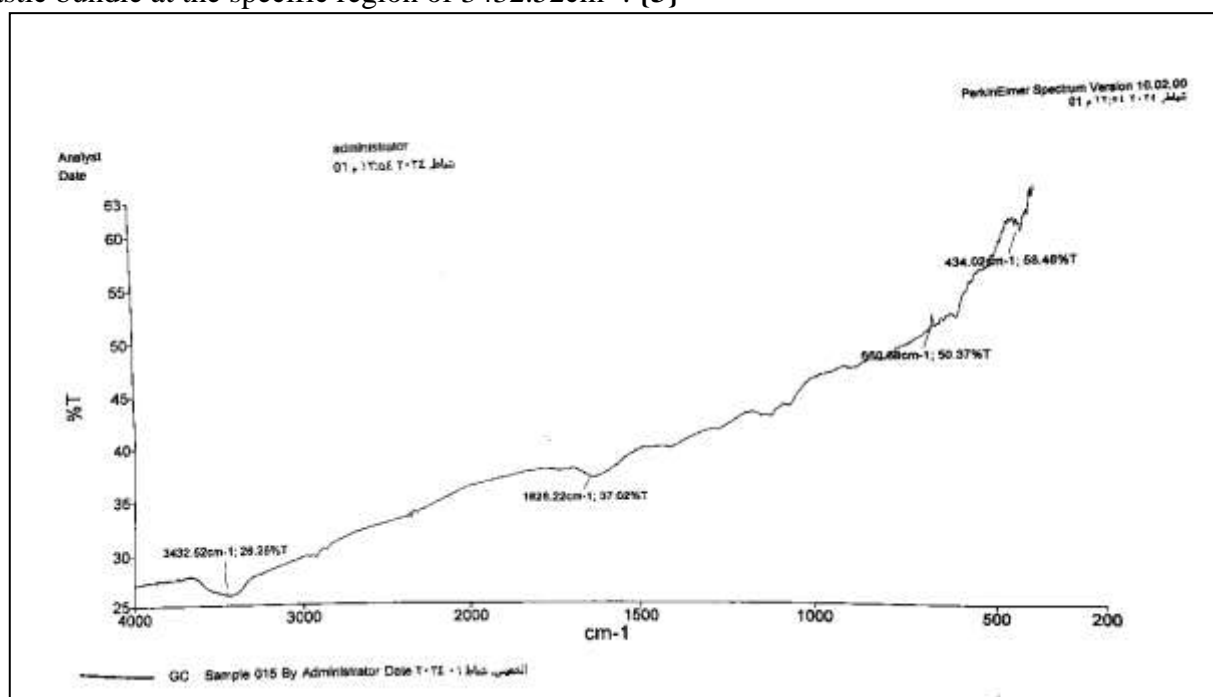


(Figure 11) infrared spectrum of the (GO/CuO)

### XRD (X-ray diffraction)

#### XRD (GO)

figure (12) shows the basic peaks of the x-ray diffraction curves of the prepared graphene oxide, as we notice the appearance of two clear peaks, showed that the highest values were obtained for the diffraction angles (26.49, 12.42) corresponding to the miller coefficients (001,002). It has been shown in the figure below that the graphene oxide nanoparticles are negated and contain sharp peaks indicating the presence of the functional groups (carboxylic acid, carbonyl, hydroxyl and epoxy) on the surfaces and edges of the graphene oxide sheets

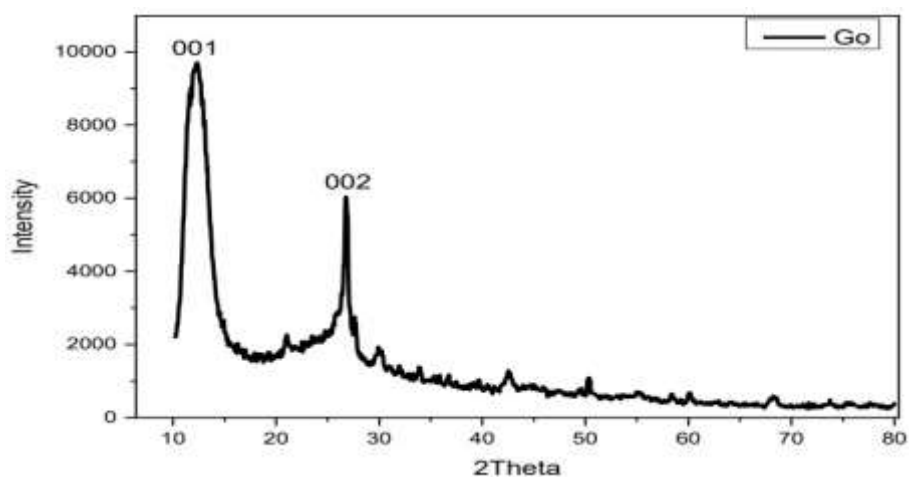


(Figure 12) XRD of the (GO)

#### XRD (CuO)

The results of the x-ray examinations deicted the secondary coer oxide, hch are shon in figure (13) . the values

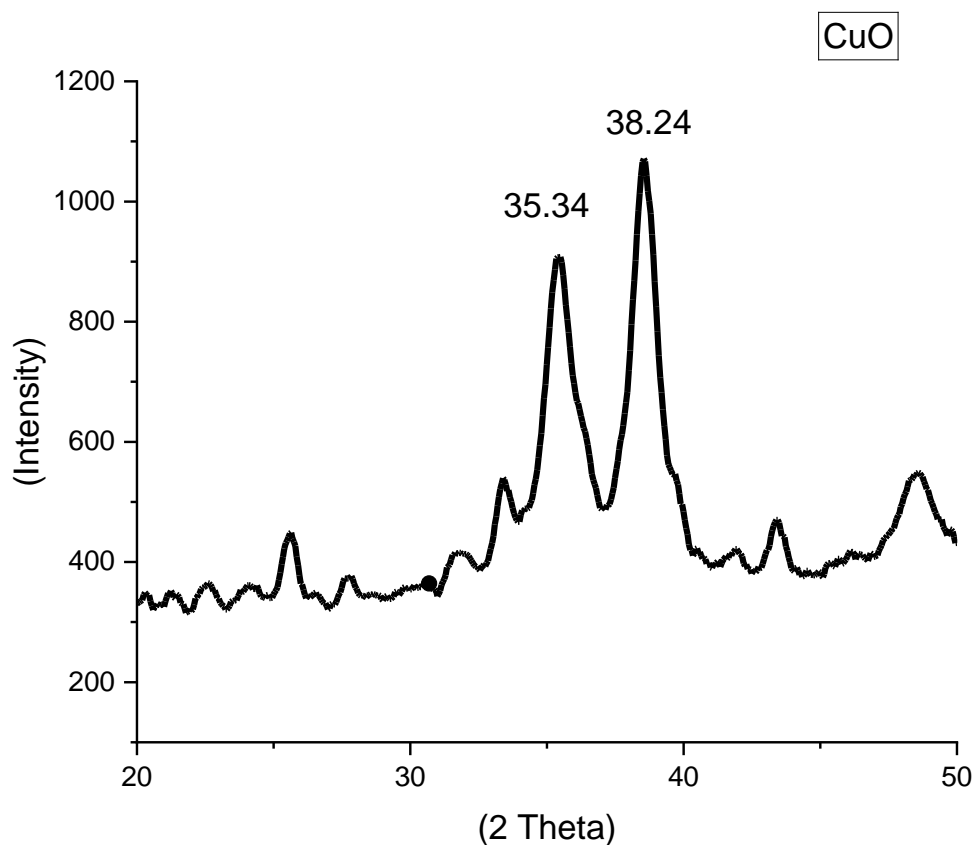


(Figure 13) XRD of the (CuO)

#### FESEM (Field Emission Electron Microscopy)

#### FESEM (GO)

(Figure 14-a) depicts a Field Emission Scanning Electron Microscope (FESEM) image of Graphene Oxide (GO) at a magnification of  $5\mu\text{m}$ . The folding and wrapping of the layer is attributed to the presence of oxygen groups on the surface. Sheet-like nanostructures were obtained. The thickness of the graphene oxide (GO) sheets varied within the range of (), as indicated by the depicted form {31}.

#### FESEM (CuO)

Field Emission Scanning Electron Microscopy (FESEM) characterized the morphology of the produced CuO nanoparticles. The figure (14-b) displays the morphological structure of CuO, magnified at a scale of  $1\mu\text{m}$ . The CuO-NPS exhibit a highly aggregated structure and possess a nearly spherical appearance. The synthesized NPS had a particle size of  $27.65\text{nm}$ .

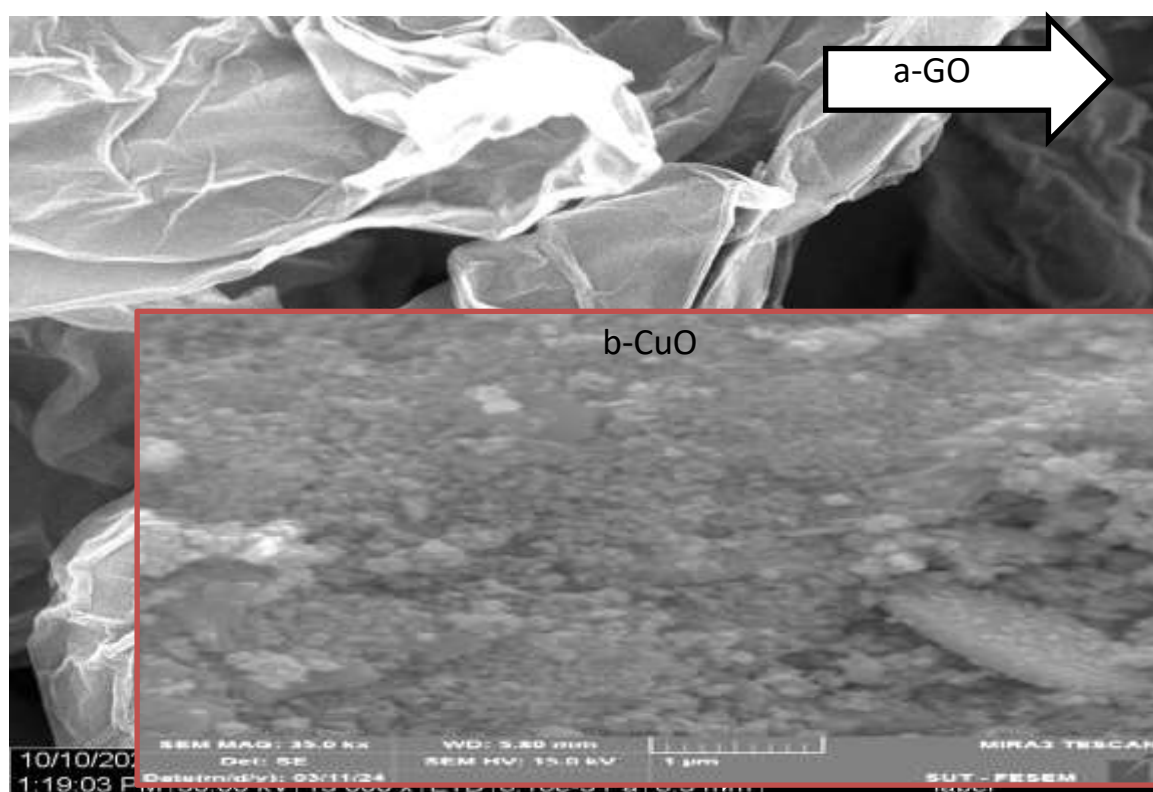


(Figure14) FESEM images of the (a-GO, b-CuO)

#### Reference

- [1] Fozia,A. Baharullah,K . Muhammad,Q. Riza,U. Mohammed,B. Anadil,G. Saira,Z. & Rizwan,A. (2021) " Green Synthesis of Copper Oxide Nanoparticles Using Aerva javanica Leaf Extract and Their Characterization and Investigation of In Vitro Antimicrobial Potential and Cytotoxic Activities " NIH.
- [2] K. Ramesh, A. Vijay, and V. Suresh Kumar, "The MIC and MBC of silver nanoparticles against Enterococcus faecalis A facultative anaerobe," Journal of Nanomedicin and Nanotechnology, vol. 6, p. 3, 2015
- [3] Khayatian, G., Jodan, M., Hassanpoor, S. and Mohebbi, S., (2016). "Determination of trace amounts of cadmium, copper and nickel in environmental water and food samples using GO/MgO nanocomposite as a new sorbent". Journal of the Iranian Chemical Society, 13(5), pp.831-839.
- [4] Hill, M.K., (2020). "Understanding environmental pollution". Cambridge University Press
- [5] Schultz, R.A. ed., (2013)." Technology versus Ecology: Human Superiority and the Ongoing Conflict with Nature: Human Superiority and the Ongoing Conflict with Nature. IGI Global



- [6] Blázquez, G., Calero, M., Hernáinz, F., Tenorio, G., and Martín-Lara, M. A. (2010). "Equilibrium biosorption of lead (II) from aqueous solutions by solid waste from olive-oil production". *Chemical Engineering Journal*, 160(2) : 615-622.
- [7] Khan, S.B.,(2011) "*Exploration of CeO<sub>2</sub> nanoparticles as a chemi-sensor and photo-catalyst for environmental applications*". *Science of the total Environment*, :(15)409.pp. (2987-2992).
- [8] Rafiq, A., Ikram, M., Ali, S., Niaz, F., Khan, M., Khan, Q., & Maqbool, M. (2021)." Photocatalytic degradation of dyes using semiconductor photocatalysts to clean industrial water pollution". *Journal of Industrial and Engineering Chemistry*, 97, 111–128.
- [9] Khan, F. S. A., Mubarak, N. M., Tan, Y. H., Khalid, M., Karri, R. R., Walvekar, R., ... & Mazari, S. A. (2021). A comprehensive review on magnetic carbon nanotubes and carbon nanotube-based buckypaper for removal of heavy metals and dyes. *Journal of Hazardous Materials*, 413, 125375.
- [10] Baughman, G. L., and Perenich, T. A. (1988). Fate of dyes in aquatic systems: I. Solubility and partitioning of some hydrophobic dyes and related compounds. *Environmental Toxicology and Chemistry: An International Journal*, 7(3),pp 183-199
- [11] Muthukumaran, C., Sivakumar, V. M., & Thirumarimurugan, M. (2016). "Adsorption isotherms and kinetic studies of crystal violet dye removal from aqueous solution using surfactant modified magnetic nanoadsorbent". *Journal of the Taiwan Institute of Chemical Engineers*, 63, 354–362
- [12] Aljamali, N. M., Aldujaili, R. A. B., & Alfatlawi, I. O. (2021). "Physical and Chemical Adsorption and its Applications". *International Journal of Thermodynamics and Chemical Kinetics*, 7(2), 1-9.
- [13] Webb, P. a. (2003). "Introduction to Chemical Adsorption Analytical Techniques and their Applications to Catalysis". MIC Technical Publications, 13(January), 1–4.
- [14] Silbey, R.J., Alberty, R.A., and Bawendi, M.G. (2005). *Physical chemistry*. 4th ed. John Wiley & Sons, Inc.
- [15] Malinauskiene, L., Zimerson, E., Bruze, M., Ryberg, K., & Isaksson, M. (2012). Patch testing with the textile dyes Disperse Orange 1 and Disperse Yellow 3 and some of their potential metabolites, and simultaneous reactions to para-amino compounds. *Contact Dermatitis*, 67(3), 130-14
- [16] Bessashia, W., *Removal of basic fuchsin from water by using mussel powdered eggshell membrane as novel bioadsorbent equilibrium, kinetics, and thermodynamic studies. Environmental research*, 2020. 186: p. (109484).
- [17] Raval, N.P., P.U. Shah, and N.K. Shah, *Malachite green "a cationic dye" and its removal from aqueous solution by adsorption. Applied Water Science*, 2017. 7(7): pp. (3407-3445).
- [18] P., Stragliotto, F., Luque, G.L.: (2021) "Effect of functionalization on graphenic surfaces in their properties. In: Nanostructured Multifunctional Materials Synthesis, Characterization, Applications and Computational Simulation, pp. 189–212. CRC Press.
- [19] Jishnu, A., Jayan, J.S., Saritha, A., Sethulekshmi, A.S., Venu, G.: (2020) "Superhydrophobic graphene-based materials with self-cleaning and anticorrosion performance: an appraisal of neoteric advancement and future perspectives". *Colloids Surf., A* 606, 125395.
- [20] Javaherdashti, R. Sarjahani, R.:(2021) "An overview of the effect of graphene as a metal protector against microbiologically influenced corrosion (MIC). *Corrosion Protection of Metals and Alloys Using Graphene and Biopolymer Based Nanocomposites*, pp. 149–168.
- [21] Ijaz, F., Shahid, S., Khan, S.A., Ahmad, W., and Zaman, S. (2017)." Green synthesis of copper oxide nanoparticles using abutilon indicum leaf extract: antimicrobial, antioxidant and photocatalytic dye degradation activities". *Tropical Journal of Pharmaceutical Research*, 16 (4), 743-753.
- [22] Singh, J., Kaur, G., and Rawat, M. (2016). "A brief review on synthesis and characterization of copper oxide nanoparticles and its applications". *Journal Bioelectron Nanotechnol*, 1 (1), 1- 9.
- [23] Iravani, S. (2011). Green synthesis of metal nanoparticles using plants. *Green Chemistry*, 13 (10), 2638-2650.
- [24] Saif, S., Tahir, A., Asim, T., and Chen, Y. (2016). Plant mediated green synthesis of CuO nanoparticles: comparison of toxicity of engineered and plant mediated CuO nanoparticles towards daphnia magna. *Nanomaterials*, 6 (11), 1-15.

- [25] Awwad, A.M., Albiss, B.A., and Salem, N.M. (2015). Antibacterial activity of synthesized copper oxide nanoparticles using *Malva sylvestris* leaf extract. *SMU Medical Journal*, 2 (1), 91-101.
- [26] Mondal, M. K., Singh, S., Umareddy, M., & Dasgupta, B. (2010). "Removal of Orange G from aqueous solution by hematite: Isotherm and mass transfer studies. *Korean Journal of Chemical Engineering*, 27(6), 1811-1815.
- [27] Arulkumar, M., Sathishkumar, P., & Palvannan, T. (2011). "Optimization of Orange G dye adsorption by activated carbon of *Thespesia populnea* pods using response surface methodology". *Journal of hazardous materials*, 186(1), 827-834.
- [28] Hummers, William S:Offeman, Richard E. (March 20, 1958).
- [29] (Preparation of Graphitic Oxide) . *Journal of the American Chemical Society*. 80 (6);1339.
- [30] Alheety, N.F., Majeed, A.H., Alheety, M.A.: (2019) "Silver nanoparticles anchored 5-methoxy benzimidazol thiomethanol (MBITM): Modulate, characterization and comparative studies on MBITM and Ag-MBITM antibacterial activities. *J. Phys. Conf. Ser.* 1294(5), 052026.
- [31] Hariprasad, S., Susheela Bai, G., Santhoshkumar, J., Madhu, C., and Sravani, D. (2016). "Greensynthesis of copper nanoparticles by are- valanata leaves extract and their anti-microbial activites". *International Journal of ChemTech Research*, 9 (2), 98-105.
- [32] Abdulwahhab,H.M. (2020). *Preparation and character of graphen and graphene oxide polymeric nanocomposites; study some of their application*.PHD.thesis university of Tikrit.
- [33] El Haddad, M., (2016) " Removal of Basic Fuchsin dye from water using mussel shell biomass waste as an adsorbent: Equilibrium, kinetics, and thermodynamics". *Journal of Taibah University for Science*. 10(5): pp. (664-674).
- [34] Heidarizad, M. and S.S. Şengör, (2016) "Synthesis of graphene oxide/magnesium oxide nanocomposites with high-rate adsorption of methylene blue". *Journal of Molecular Liquids*. 224:PP.(607-617).
- [35] Kumari, H. J., Krishnamoorthy, P., Arumugam, T. K., Radhakrishnan, S., & Vasudevan, D. (2017). An efficient removal of crystal violet dye from waste water by adsorption onto TLAC/Chitosan composite: a novel low cost adsorbent. *International journal of biological macromolecules*, 96, 324-333.
- [36] Jaeger, S., Dos Santos, A., Fernandes, A. N., & Almeida, C. A. P. (2015). Removal of p-nitrophenol from aqueous solution using Brazilian peat: kinetic and thermodynamic studies. *Water, Air, & Soil Pollution*, 226(8), 1-12.
- [37] Tran, H. N., You, S. J., & Chao, H. P. (2016). Thermodynamic parameters of cadmium adsorption onto orange peel calculated from various methods: A comparison study. *Journal of Environmental Chemical Engineering*, 4(3), 2671– 2682..